2009

Site-specific covalent attachment of DNA to proteins using a photoactivatable Tus-Ter complex

Dahdah B. Dahdah
James Cook University

Isabelle Morin
James Cook University

Morgane Moreau
James Cook University

Nicholas E. Dixon
University of Wollongong, nickd@uow.edu.au

Patrick M. Schaeffer
James Cook University

Site-specific covalent attachment of DNA to proteins using a photoactivatable Tus-Ter complex

Abstract

Investigations into the photocrosslinking kinetics of the protein Tus with various bromodeoxyuridine-substituted Ter DNA variants highlight the potential use of this complex as a photoactivatable connector between proteins of interest and specific DNA sequences.

Keywords

Site, specific, covalent, attachment, DNA, proteins, using, photoactivatable, Tus, Ter, complex

Disciplines

Life Sciences | Physical Sciences and Mathematics | Social and Behavioral Sciences

Publication Details

Dahdah, D. B., Morin, I., Moreau, M., Dixon, N. E. & Schaeffer, P. M. (2009). Site-specific covalent attachment of DNA to proteins using a photoactivatable Tus-Ter complex. Chemical Communications: Chemcomm, (21), 3050-3052.

Site-specific covalent attachment of DNA to proteins using a photoactivatable Tus–*Ter* complex†

Dahdah B. Dahdah,‡[a] Isabelle Morin,‡[a] Morgane J. J. Moreau,[a] Nicholas E. Dixon[b] and Patrick M. Schaeffer*[a]

Received (in Cambridge, UK) 15th January 2009, Accepted 17th March 2009
First published as an Advance Article on the web 9th April 2009
DOI: 10.1039/b900905a

Investigations into the photocrosslinking kinetics of the protein Tus with various bromodeoxyuridine-substituted *Ter* DNA variants highlight the potential use of this complex as a photoactivatable connector between proteins of interest and specific DNA sequences.

Artificial DNA–protein conjugates have recently attracted attention as tools for nanobiotechnology and bioanalytical chemistry. Their utility as biosensors, artificial nucleases or in protein microarrays has been successfully demonstrated.[1] Various systems for the covalent attachment of proteins to nucleic acids have been described, including chemical crosslinking of oligonucleotides to protein lysine or cysteine residues,[2] expressed protein ligation,[1c,3] chemoenzymatic reactions[4] and the use of photoaptamers.[5] The objective of this work was to develop a straightforward and reliable method to covalently and regiospecifically link any protein of interest (POI) with any specific DNA sequence. To do so, we made use of the DNA-binding properties of the 36 kDa *Escherichia coli* replication terminator protein Tus.

In *E. coli*, chromosomal DNA replication proceeds bidirectionally from the origin, and the two replication forks meet in the terminus region,[6] which contains ten 23-bp *Ter* sites (*TerA–J*) arranged in two oppositely-oriented groups of five.[7] Each *Ter* site binds Tus.[8] A replication fork can pass through the first group of Tus-bound *Ter* sites, where it encounters the "permissive" face of the Tus–*Ter* complex, but is stopped by the second group where it now encounters the non-permissive face. A recent study revealed the mechanism for this obvious polarity of fork arrest.[9] The rates of dissociation of Tus from forked *TerB* oligonucleotides, such as those produced by the replicative DnaB helicase, at both the non-permissive and permissive ends of the *Ter* site were measured by SPR, which demonstrated that melting of the strictly conserved G–C(6) base pair at the non-permissive end led to formation of a much more stable "locked" Tus–*TerB* complex (TT-Lock). The crystal structure of the locked complex showed that C(6) moves ~14 Å to bind in a cytosine-specific pocket on the surface of Tus. Many of the conserved residues among the various *Ter* sites make base-specific contacts with Tus and a large number of other non-specific contacts are electrostatic.[9,10] The dissociation constant (K_D) of Tus–*TerB* was reported to be 0.3 pM in 0.15 M potassium glutamate, and its half-life was more than 9 h.[11] The binding of this complex is strongly dependent on ionic strength, with the value of K_D rising to about 1 nM, and the half-life decreasing to about 2 min, in a buffer containing 0.25 M KCl.[9,12]

Protein–DNA complexes can be studied by photochemical cross-linking of proteins to 5-halogenated (deoxy)uridine (*e.g.*, BrdU, IdU) substituted nucleic acids.[13] A proposed mechanism involves formation of a reactive C-centred radical by homolytic cleavage of the carbon–halogen bond of 5-halouracil.[14] The photoreactivity of these analogues was utilized to crosslink Tus to *TerB* DNA by substituting T(8) for 5-BrdU.[15] However, efficiency was only 15%, even with lengthy UV irradiation. Trypsin digestion of Tus revealed a crosslinked segment that matched residues 122–139. The crystal structure of the TT-Lock showed that residues in the unpaired region at the non-permissive face occupy radically different positions to those in the fully double-stranded Tus–*TerA* structure.[9] In particular, and consistent with predictions from biochemical data, the major differences between the structures of the DNA ligands involve strand separation at residues preceding T-A(7), with C(6) binding in the cytosine binding pocket of Tus near helix α4 (residues 135–147).[9] The T-A(7) base pair makes no base-specific contacts in the structures, but is disrupted in the TT-Lock, with A(7) stacking on the face of the phenyl ring of Phe140. We hypothesized that *Ter* sequences that are able to form locked complexes and contain a BrdU substitution at position A(7) could, upon photochemical activation, be crosslinked in high yields with helix α4 of Tus. Our primary objective was to optimize photocrosslinking. We reasoned that the structure of *Ter* variants (Fig. 1A) could influence the kinetics and reaction yields depending on their ability to form a TT-Lock. The *Ter* variants Br/P1 and Br/P4 do not form the TT-Lock as C(6) of *Ter* is base paired, whereas Br/P2, Br/P3 and Br/P5 will do so, since C(6) is not base paired.

To ensure that Tus forms stoichiometric complexes with the *Ter* variants, a modified electrophoretic mobility shift assay (EMSA) was used to demonstrate the differential migration of free Tus compared to Tus–*Ter* complexes. The complexes were prepared using N-terminally His_6-tagged Tus. Stoichiometric

[a] *Comparative Genomics Centre, School of Pharmacy & Molecular Sciences, James Cook University, DB 21, James Cook Drive, Townsville, QLD 4811, Australia. E-mail: Patrick.Schaeffer@jcu.edu.au; Fax: +61 (0)7 47816078; Tel: +61 (0)7 47814448*
[b] *School of Chemistry, University of Wollongong, Building 18, Northfields Avenue, NSW 2522, Australia*

† Electronic Supplementary Information (ESI) available: Experimental details. See DOI: 10.1039/b900905a/

‡ Authors contributed equally to this work. This work was supported by a grant from the National Health and Medical Research Council.

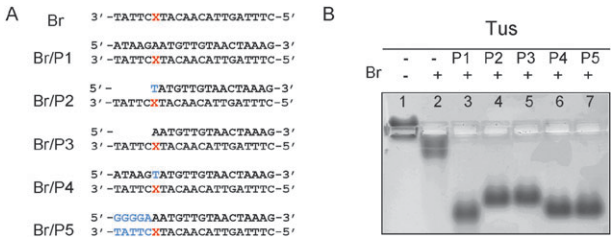

Fig. 1 A. Sequences of *Ter* oligonucleotides. BrdU substitution is in red. Mismatched bases are in blue. B. EMSA in TBE-agarose of the Tus–*Ter* variant complexes (25 μM). Free and DNA-bound proteins were visualized by Coomassie blue staining.

mixtures of His_6-Tus and *Ter* variants were electrophoretically separated on an agarose gel (Fig. 1B). All Tus–*Ter* complexes migrate towards the anode due to the presence of negatively charged oligonucleotides bound to Tus (lanes 3 to 7) when compared to free Tus (lane 1). In lanes 3–7, the presence of only one band demonstrates that Tus binds stoichiometrically to all *Ter* variants. Lane 2 represents the weak (non-specific) interaction of Tus with the Br oligonucleotide. In this case, Tus progressively dissociates from Br, resulting in a smear. The difference in migration observed in lanes 4 and 5 compared to lanes 3, 6 and 7 is due to the difference in size of the bound *Ter* variants.

In the next stage, we evaluated the photocrosslinking kinetics with preformed Tus–*Ter* complexes. Drops of the complex were spotted under the cover of an ice-cold 96-well plate and irradiated using a UV-transilluminator set at 312 nm (Vilber Lourmat); drops were hanging ~7 mm above the surface of the transilluminator. The yield of crosslinking was assessed by SDS-PAGE followed by Coomassie blue staining (Fig. 2A). The upper band, appearing over time, corresponds to the photocrosslinked Tus–*Ter* variants. The yields for crosslinked Br/P2, Br/P3 and Br/P5 were similar, at around 60–65% after 9 min (Fig. 2B). Their first order reaction rate constants (k) were also similar, ranging from 0.19 to 0.26 min^{-1}. Surprisingly, k for Br/P1 and Br/P4 were >4-fold higher, at 1.2 and 1.4 min^{-1} respectively, though the yields were lower (32–46%) than for the TT-Lock forming Br/P2, Br/P3 and Br/P5 species. Finally, as expected, very weak crosslinking was observed for the Br-Tus complex, but it occurred with a similar k value to that obtained with the TT-Lock forming variants; this suggests that the reaction rate is influenced by C(6) not being base paired.

Since we intend later to crosslink Tus to *Ter* sequences at the ends of longer DNAs, the salt dependence of the crosslinking reaction was studied to ensure that it would still occur efficiently under conditions where non-specific Tus–DNA interactions are not observed (>0.2 M KCl).[12] Increasing the ionic strength disrupts electrostatic interactions in both the Tus–*Ter* and non-specific Tus–DNA complexes,[9,12] and could also affect the photocrosslinking reaction. To evaluate this, each *Ter* variant was treated with Tus in increasing concentrations of KCl and irradiated for 6 min. Crosslinking efficiency was quantified as before (Fig. 3A). Here we expected that, at some point, the KCl concentration would weaken the ability of Tus to form a complex with the *Ter* variants, resulting in more unbound Tus. As a consequence, less crosslinking would occur and this would be directly related to the K_D of the complexes. As expected, the most stable complexes were obtained for the TT-Lock forming species Br/P2 and Br/P3, as shown by the persistence of the crosslinked fraction at 0.85 and 0.95 M KCl. The salt did not apparently affect the photochemistry, with respect to rates or yields. Data were fit to a sigmoidal dose-response model where IC_{50} values indicate salt concentrations necessary to achieve a 50% reduction in the yield obtained in low salt conditions after 6 min of UV irradiation. For Br/P2 and Br/P3 the IC_{50} values of 0.66 and 0.70 M correlated well with high complex stability (Fig. 3B). For Br/P1 and Br/P4, IC_{50} values of 0.47 and 0.50 M, respectively, are consistent with the lower stability of these complexes. Tus also bound non-specifically to Br in low salt, but the complex was totally disrupted by 0.25 M KCl. However, unexpected results were obtained for Br/P5. Despite its ability to form the TT-Lock, this complex was less stable,

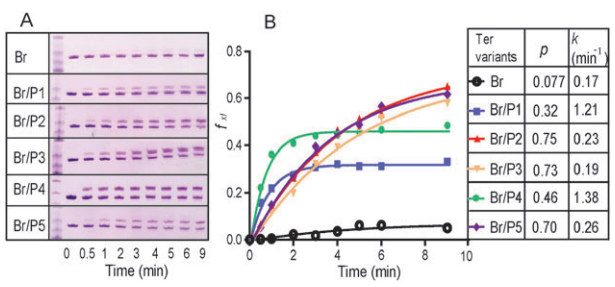

Fig. 2 Crosslinking reaction kinetics. A. Tus proteins (2 μl at 50 μM in 50 mM phosphate, pH 7.8) and *Ter* variants (2 μl at 50 μM in 10 mM Tris, pH 8, 125 mM KCl) were mixed and UV-irradiated for the times indicated. Proteins were separated by SDS-PAGE and visualized by Coomassie blue staining. The retarded bands correspond to the crosslinked Tus–*Ter* complexes. B. The fractions of crosslinked Tus–*Ter* complexes were quantified using ImageJ software. The data were fit to a simple first order rate expression for product formation: $f_{xl} = p(1 - e^{-kt})$, where f_{xl} is the fraction of crosslinked product, p is the theoretical plateau, t is time and k is the rate constant.[5c] The table lists p and k values for each of the *Ter* variants.

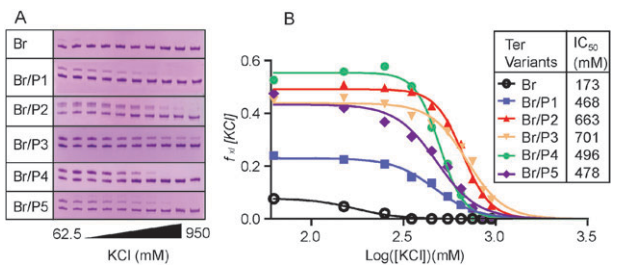

Fig. 3 Ionic strength dependence of crosslinking of the Tus–*Ter* complexes. A. *Ter* variants were treated with Tus in increasing KCl concentrations from 62.5 to 950 mM and UV irradiated for 6 min. Proteins were separated by SDS-PAGE and visualized with Coomassie blue. The retarded bands correspond to the crosslinked product at each KCl concentration, giving fractional yields, $f_{xl[KCl]}$. B. The $f_{xl[KCl]}$ were quantified using ImageJ software and the data were fit to a sigmoidal dose-response model with the bottom plateau value set to zero and a variable slope: $f_{xl[KCl]} = T/(1 + 10^{((\log IC50 - [KCl])\sigma)})$, where T is the top plateau value, IC_{50} is the 50% inhibitory concentration, and σ is the Hill slope. The table lists IC_{50} values for each of the *Ter* variants.

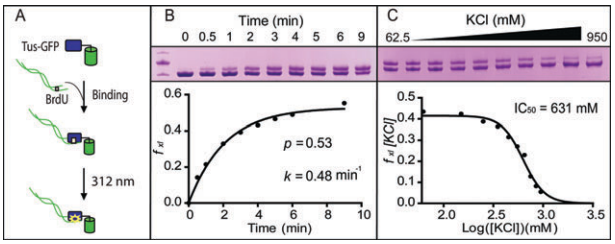

Fig. 4 Tus as a connector for the production of covalent GFP–DNA conjugates. A. Reaction scheme for TusGFP–Br/P2 synthesis. B. Crosslinking reaction kinetics. TusGFP was mixed with Br/P2 and UV irradiated for the times indicated. Electrophoresis and quantification of f_{xl} were as described in Fig. 2. C. Ionic strength dependence of the TusGFP–Br/P2 complex. TusGFP and Br/P2 were mixed in increasing KCl concentrations and UV-irradiated for 6 min. Electrophoresis and quantification of $f_{xl[KCl]}$ were as described in Fig. 3.

with an IC_{50} value of 0.48 M. In these reactions, we observed that concentrations of KCl ranging from 0.15–0.65 M generated unexpected bands of higher molecular weights (Fig. 3A). We believe that the presence of these bands may affect the quantification of crosslinking and consequently the IC_{50} value. These bands were specifically observed for Br/P5 *Ter* variants and were not investigated further.

Finally, we tested the use of Tus as a fusion tag to covalently and site-specifically link a POI to DNA containing the photoactivatable Br/P2 sequence. As a proof-of-principle study, we chose green fluorescent protein (GFP) as our POI (Fig. 4A). His_6-tagged TusGFP fusion protein were expressed, purified and mixed with stoichiometric amounts of Br/P2.

TusGFP stoichiometrically bound to Br/P2, confirming that the function of Tus in the fusion protein is not compromised (see ESI†). Kinetic studies of the UV-irradiated TusGFP–Br/P2 complex revealed successful crosslinking as demonstrated by the appearance of one upper band (Fig. 4B). The photocrosslinking kinetics were similar to those for Tus–Br/P2, with $p = 0.53$ and $k = 0.48$ min^{-1}. Thus, fusion of GFP to Tus does not strongly affect the crosslinking reaction with Br/P2. Salt dependence experiments indicated that the TusGFP–*Ter* complex is highly stable, and residual crosslinking still occurred at KCl concentrations as high as 0.95 M; IC_{50} = 0.63 M (Fig. 4C). Reaction rates were not much affected by ionic strength. This flexibility is advantageous for use of the system in downstream applications.

Further investigations are required to show if Phe140 is involved in covalent bond formation. Large k values and high yields were expected with the TT-Lock complexes and slow reaction rates and low yields were expected for complexes with base-paired G–C(6), which is in sharp contrast with our results. Nevertheless, the difference in yield observed between the different species still suggests that the formation of the TT-Lock is necessary to avoid non-productive photoreactions that would result in fewer crosslinking events.

In conclusion, we have demonstrated for the first time that Tus in combination with Br/P2 or Br/P3 *Ter* variants that are able to form the TT-Lock can be used as an efficient connector system for the site-specific synthesis of covalent protein–DNA conjugates under very mild conditions without extensive purification steps. To our knowledge, this is the first account of large scale synthesis (reactions were done at concentrations of 25 μM) of covalent fusion protein–DNA conjugates using a photocrosslinking method, and the scale of synthesis can easily be further increased. The reactions can be carried out simply with a UV-transilluminator to achieve up to 65% yield of covalent bond formation (Br/P2) in just 9 min. We demonstrated that exposure at 312 nm, which is in the tail of the absorption spectrum of BrdU,[14b] can be efficiently used to avoid DNA-damage (see ESI†). Crosslinking can be done in moderate to high salt conditions without affecting the reaction rates, thereby providing flexibility in reaction conditions. The procedure affords stoichiometric protein–DNA conjugates with well-defined regiospecificity. Another advantage is that the reactions can be carried out at very low concentrations due to the high affinity (K_D < nM) of these species. Finally, due to its simplicity, speed, flexibility and robustness, we expect this procedure to be useful in many applications requiring the production of covalent protein–DNA conjugates such as proteomics, molecular diagnostics and nanotechnology.

Notes and references

1 (*a*) C. M. Niemeyer, *Trends Biotechnol.*, 2002, **20**, 395–401; (*b*) M. Lovrinovic, M. Spengler, C. Deutsch and C. M. Niemeyer, *Mol. Biosyst.*, 2005, **1**, 64–69; (*c*) I. Burbulis, K. Yamaguchi, A. Gordon, R. Carlson and R. Brent, *Nat. Methods*, 2005, **2**, 31–37; (*d*) S. Takeda, S. Tsukiji, H. Ueda and T. Nagamune, *Org. Biomol. Chem.*, 2008, **6**, 2187–2194.

2 (*a*) E. R. Hendrickson, T. M. H. Truby, R. D. Joerger, W. R. Majarian and R. C. Ebersole, *Nucleic Acids Res.*, 1995, **23**, 522–529; (*b*) D. R. Corey and P. G. Schultz, *Science*, 1987, **238**, 1401–1403.

3 M. Lovrinovic, L. Fruk, H. Schroder and C. M. Niemeyer, *Chem. Commun.*, 2007, 353–355.

4 (*a*) M. Humenik, Y. W. Huang, Y. R. Wang and M. Sprinzl, *ChemBioChem*, 2007, **8**, 1103–1106; (*b*) B. P. Duckworth, Y. Chen, J. W. Wollack, Y. Sham, J. D. Mueller, T. A. Taton and M. D. Distefano, *Angew. Chem., Int. Ed.*, 2007, **46**, 8819–8822.

5 (*a*) H. Petach and L. Gold, *Curr. Opin. Biotechnol.*, 2002, **13**, 309–314; (*b*) C. Bock, M. Coleman, B. Collins, J. Davis, G. Foulds, L. Gold, C. Greef, J. Heil, J. S. Heilig, B. Hicke, M. N. Hurst, G. M. Husar, D. Miller, R. Ostroff, H. Petach, D. Schneider, B. Vant-Hull, S. Waugh, A. Weiss, S. K. Wilcox and D. Zichi, *Proteomics*, 2004, **4**, 609–618; (*c*) T. H. Koch, D. Smith, E. Tabacman and D. A. Zichi, *J. Mol. Biol.*, 2004, **336**, 1159–1173.

6 P. M. Schaeffer, M. J. Headlam and N. E. Dixon, *IUBMB Life*, 2005, **57**, 5–12.

7 F. F. Coskun-Ari and T. M. Hill, *J. Biol. Chem.*, 1997, **272**, 26448–26456.

8 C. Neylon, A. V. Kralicek, T. M. Hill and N. E. Dixon, *Microbiol. Mol. Biol. Rev.*, 2005, **69**, 501–526.

9 M. D. Mulcair, P. M. Schaeffer, A. J. Oakley, H. F. Cross, C. Neylon, T. M. Hill and N. E. Dixon, *Cell*, 2006, **125**, 1309–1319.

10 K. Kamada, T. Horiuchi, K. Ohsumi, N. Shimamoto and K. Morikawa, *Nature*, 1996, **383**, 598–603.

11 P. A. Gottlieb, S. Wu, X. Zhang, M. Tecklenburg, P. Kuempel and T. M. Hill, *J. Biol. Chem.*, 1992, **267**, 7434–7443.

12 C. Neylon, S. E. Brown, A. V. Kralicek, C. S. Miles, C. A. Love and N. E. Dixon, *Biochemistry*, 2000, **39**, 11989–11999.

13 (*a*) H. Steen, J. Petersen, M. Mann and O. N. Jensen, *Protein Sci.*, 2001, **10**, 1989–2001; (*b*) K. M. Meisenheimer and T. H. Koch, *Crit. Rev. Biochem. Mol. Biol.*, 1997, **32**, 101–140.

14 (*a*) C. R. Wang and Q. B. Lu, *Angew. Chem., Int. Ed.*, 2007, **46**, 6316–6320; (*b*) C. L. Norris, P. L. Meisenheimer and T. H. Koch, *J. Am. Chem. Soc.*, 1996, **118**, 5796–5803; (*c*) C. L. Norris, K. M. Meisenheimer and T. H. Koch, *Photochem. Photobiol.*, 1997, **65**, 201–207.

15 L. J. Duggan, P. T. Asmann, T. M. Hill and P. A. Gottlieb, *Biochemistry*, 1996, **35**, 15391–15396.